Optical activity in an artificial chiral media: a terahertz time-domain investigation of Karl F. Lindman's 1920 pioneering experiment

A. Y. Elezzabi* and S. Sederberg

Ultrafast Photonics and Nano-Optics Laboratory
Department of Electrical and Computer Engineering, University of Alberta
Edmonton, Alberta, Canada T6G 2V4
**Corresponding author: elezzabi@ece.ualberta.ca*

Abstract: Chiral media interact preferentially with either left- or right-circularly polarized electromagnetic waves, leading to effects including circular dichroism, optical rotation and circular preferential scattering. In this experiment, we revisit Lindman's famous 1920 experiment linking artificial chiral materials to optical activity and we record the first time-domain measurements of a single-cycle THz pulse transmitted through randomly oriented metallic helices. Time-resolved measurements of co- and cross-polarized components of the transmitted electric field allow the electric field trajectory to be reconstructed and time dynamics of the two circular components to be investigated. For the first time, we show that time dynamics reveal two distinct effects that are separated in time: local preferential circular scattering and collective coupling. These findings are important on furthering our understanding on the analogy between optical activity arising from light interaction with large chiral molecules and that from macroscopic artificial chiral media.

OCIS codes: (300.6495) Spectroscopy, terahertz; (320-7100) Ultrafast measurements; (260.5430) Polarization; (300.6530) Spectroscopy, ultrafast

References and links

1. D. F. Arago, "Mémoire sur une modification remarquable qu`éprouvent les rayons lumineux dans leur passage a` travers certains corps diaphanes, et sue quelques autres nouveaux phénoménes d`optique," Mém. Sci. Math. Phys. Inst. **1**, 93-134 (1811).
2. J. B. Biot, "Mémoire sur un nouveau genre d`oscillation que les molécules de la lumiére éprouvent en traversant certains cristaux" Mém. Sci. Math. Phys. Inst. **1**, 1-372 (1812).
3. L. Pasteur, "Sur les relations qui peuvent exister entre la forme cristalline, la composition chimique et le sens de la polarisation rotatoire," Ann. Chimie et Physique. **24**, 442-459 (1848).
4. J. C. Bose, "On the rotation of plane of polarisation of electric waves by a twisted structure," Proc. R Soc. Lond. A **63**, 146-152, (1898).
5. K. F. Lindman, "Über eine durch ein isotropes System von spiralförmigen Resonatoren erzeugte Rotationspolarization der elektromagnetische Wellen," Annalen der Physik **63**, 621-644 (1920).
6. M. H. Winkler, "An experimental investigation of some models for optical activity," J. Phys. Chem. **60**, 1656-1659 (1956).
7. I. Tinoco Jr. and M. P. Freeman, "The optical activity of oriented copper helices. I. Experimental," J. Phys. Chem. **61**, 1196-1200 (1957).
8. S. F. Mason, "Optical Activity and Molecular Dissymmetry" Contemp. Phys. **9**, 239-256, (1968).
9. L. D. Barron, *Molecular Light Scattering and Optical Activity* (Cambridge Univ. Press, Cambridge 1982).
10. J. H. Brewster, "Helix models for optical activity" in *Topics in Stereochemistry*, vol. 2, 1-72, N. L. Allinger and E. L. Eliel, ed. (John Wiley & Sons, Inc., 1967).
11. F. Dufey, "Optical activity in the Drude helix" Chem. Phys. **330**, 326-332 (2006).
12. S. F. Mason, *Molecular Optical Activity and the Chiral Discriminations* (Cambridge University Press, Cambridge, 1982).

#108071 - $15.00 USD Received 26 Feb 2009; revised 31 Mar 2009; accepted 31 Mar 2009; published 6 Apr 2009

13. I. Tinoco Jr. and A. L. Williams Jr., "Differential absorption and differential scattering of circularly polarized light: applications to biological molecules," Annu. Rev. Phys. Chem. **35**, 329-355 (1984).
14. I. Tinoco Jr., C. C. Bustamante, and M. F. Maestre, "The optical activity of nucleic acids and their aggregates," Annu. Rev. Biophys. Bioeng. **9**, 107-141 (1980).
15. G. D. Fasman, *Circular dichroism and the conformational analysis of biomolecules* (Oxford University Press, Oxford, 1997).
16. I. Tinoco Jr., and A. L. Williams Jr., "Differential absorption and differential scattering of circularly polarized light," Annu. Rev. Phys. Chem. **35**, 329-355 (1984).
17. K. J. Chau, M. C. Quong, and A. Y. Elezzbi, "Terahertz time-domain investigation of axial optical activity from a sub-wavelength helix," Opt. Express **15**, 3557-3567 (2007).
18. M. H. Umari, V. V. Varadan, and V. K. Vardan, "Rotation and dichroism associated with microwave propagation in chiral composite samples," Radio Sci. **26**, 1327-1334 (1991).
19. R. Ro, V. V. Varadan, and V. K. Vardan, "Electromagnetic activity and absorption in microwave chiral composites," IEEE Proc. H **139**, 441-448 (1992).
20. V. V. Varadan, R. Ro, and V. K. Varadan, "Measurement of the electromagnetic properties of chiral composite materials in the 8-40 GHz range," Radio Sci. **29**, 9-22 (1994).
21. J. H. Cloete, M. Bingle, and D. B. Davidson, "The role of chirality and resonance in synthetic microwave absorbers," Int. J. Electron. Commun. **55**, 233-239 (2001).
22. S. Motojima, Y. Noda, S. Hoshiya, and Y. Hishikawa, "Electromagnetic wave absorption property of carbon microcoils in 12-110 GHz region" J. Appl. Phys. **94**, 2325-2330 (2003).
23. F. Guerin, P. Bannelier, and M. Labeyrie, "Scattering of electromagnetic waves by helices and application of the modelling of chiral composites. I: simple effective-medium theories," J. Phys. D **28**, 623-642 (1995).
24. F. Guerin, P. Bannelier, M. Labeyrie, J.-P. Ganne, and P. Guillon, "Scattering of electromagnetic waves by helices and applications to the modelling of chiral composites. II. Maxwell Garnett treatment," J. Phys. D **28**, 643-656 (1995).
25. F. C. F. Bohren, R. Luebbers, H. S. Langdon, and F. Hunsberger, "Microwave-absorbing chiral composites: is chirality essential or accidental," Appl. Opt. **31**, 6403-6407 (1992).
26. I. V. Lindell, A. H. Sihvola, S. A. Tretyakov, and A. J. Viitanen, *Electromagnetic Waves in Chiral and Bi-Isotropic Media.* (Artech House, Boston 1994).
27. J. F. Holzman, F. E. Vermeulen, S. E. Irvine, and A. Y. Elezzabi, "Free-space detection of terahertz radiation using crystalline and polycrystalline ZnSe electro-optic sensors," APL. **81**, 2294 (2002).
28. Mathias Johansson, "The Hilbert transform" Master Thesis, Mathematics, Växjö University (1999).
29. E. U. Condon, "Theories of optical rotary power" Rev. Mod. Phys. **9**, 432-457 (1937)
30. D. Moore and I. Tinoco Jr., "The circular dichroism of large helices. A free particle on a helix" J. Chem. Phys. **72**, 3396-3700 (1980).
31. I. Tinoco Jr. and R. Woody, "Optical rotation of oriented helices. IV a free electron on a helix," J. Chem. Phys. **40**, 160-165 (1964).
32. K. M. Flood and D. L. Jaggard, "Effective charge densities and current densities in isotropic chiral media," J. Opt. Soc. Am. A **12**, 177-183 (1995).
33. C. Bustamante, M. F. Maestre, and I. Tinoco Jr., "Circular intensity differential scattering of light by helical structures. I. Theory," J. Chem. Phys. **73**, 4273-4281 (1980).
34. C. Bustamante, M. F. Maestre, and I. Tinoco Jr., "Circular intensity differential scattering of light by helical structures. II. Applications," J. Chem. Phys. **73**, 6046-6055 (1980).
35. C. Bustamante, I. Tinoco Jr., and M. F. Maestre, "Circular intensity differential scattering of light by helical structures. III. A general polarizability tensor and anomalous scattering," J. Chem. Phys. **74,** 4839-4850 (1981).
36. C. Bustamante, I. Tinoco Jr., and M. F. Maestre, "Circular intensity differential scattering of light. IV. Randomly oriented species," J. Chem. Phys. **76**, 3440-3446 (1982).
37. C. Bustamante, I. Tinoco Jr., and M. F. Maestre, "Circular differential scattering can be an important part of the circular dichroism of macromolecules," Proc. Natl. Acad. Sci. **80**, 3568-3572 (1983).
38. M. F. Maestre, C. Bustamante, T. L. Hayes, J. A. Subirana, and I. Tinoco Jr., " Differential scattering of circularly polarized light by the helical sperm head the octopus *Eledone cirrhosa*," Nature **298**, 773-774 (1982).

1. Introduction

Optical activity or, more generally, electromagnetic activity is an intriguing phenomenon of light-matter interaction. It is observed when a chiral medium (an electromagnetically active substance) interacts with the polarization state of an electromagnetic wave and couples selectively with either the left- or right-circularly polarized (LCP or RCP) component. Since the trajectory of the electric field vector of either a LCP or a RCP light wave is effectively a

#108071 - $15.00 USD Received 26 Feb 2009; revised 31 Mar 2009; accepted 31 Mar 2009; published 6 Apr 2009

'*chiral*' vector field, the handedness of the material determines which component will couple and interact more closely with the material. Optical activity manifests itself as preferential transmission of either the LCP or RCP electric field component accompanied by an accumulation of phase between the two components. Upon traversing through a crystalline or liquid chiral medium, the component matching the handedness of the material will couple, whereas the opposite component will experience absorption and scattering. Furthermore, these two components will experience different indices of refraction and a nonzero phase difference will accumulate as the two components propagate. Thus, for interaction with a linearly polarized electromagnetic field, which can be considered as an equal superposition of a LCP and a RCP electric field, the linear electric field polarization state is transformed into an elliptical polarization state. This phenomenon is referred to as circular dichroism (CD). Accompanying this polarization transformation is preferential phase retardation or advancement between the LCP and RCP electric field components. The phase difference is due to the difference in the phase velocities or equivalently, the differences in the intrinsic refractive indices between the LCP and RCP electric fields. Consequently, the major axis of the ellipse will rotate relative to the initial direction of the incident field. The sense of rotation depends on the material handedness or its structural asymmetry. This phenomenon is known as optical rotation or as optical rotary dispersion (ORD) when measured as a function of wavelength. Notably, in a molecular chiral medium, the exhibited CR and ORD originate from the same electronic transitions and are related to one another via Kronig-Kramer relations.

The optical activity phenomenon has been a topic of investigation for almost two centuries, beginning in 1811 when Arago demonstrated its presence in quartz crystals as light propagates along the crystal's optical axis [1]. In this regard, optical activity was associated with crystalline symmetry and, in particular, with those crystals exhibiting optical birefringence. Later on, however, Biot showed that liquids can exhibit optical activity as well [2]. His discovery of the phenomenon in a medium that did not possess any specific crystalline symmetry has been important in paving the way for an innovative interpretation of the nature of optical activity. This fundamental experiment was the first to ascribe the observed optical activity to the arrangement of the individual molecules that make up the randomly-oriented liquid state. The link between optical activity and geometry was proposed by Louis Pasteur in 1849. He postulated that the optically active molecules making up tartaric acid have either helical or asymmetric tetrahedral arrangements [3], and that they are not superimposable on their mirror image by translations and rotations (i.e. they are enantiomers of each other).

Due to its wide presence in nature, the helical conformation is considered to be the most universal form of a chiral object and thus far has been the most studied optically active structure. Artificial chiral materials were studied by Bose almost a century ago [4], and he demonstrated rotation of the plane of polarization of electromagnetic waves as they traversed a jute bundle. He attributed the rotation of the plane of polarization to the twisted structure of the jute fibres. Regrettably, his pioneering work was overlooked by many scientists as being the first experimental evidence connecting chirality to optical activity. More elaborate follow-up experiments by Lindman [5], Winkler [6], and Tinoco [7], showing polarization rotation of microwave radiation transmitted through metallic helices, helped to qualitatively establish the structural similarities between macroscopic helices and microscopic optically active molecules [8-11]. Their pioneering work demonstrated that chiral composite media can be artificially constructed by embedding chiral objects with similar handedness in a dielectric host. Since the sense of polarization rotation of the transmitted electromagnetic wave was shown to adopt the handedness of the medium, the individual helices making up the chiral composites are considered to be good models for chiral macromolecules (i.e. artificial helical macromolecules).

#108071 - $15.00 USD Received 26 Feb 2009; revised 31 Mar 2009; accepted 31 Mar 2009; published 6 Apr 2009

Notably, the pioneering works of Pasteur, Bose, and others on optical activity and their considerations in linking the phenomenon to chirality have laid the foundation for our modern day understanding. Thus far, the study of chiral light-matter interaction has been an impetus for progress in biology [12-14] and biochemistry [15,16], and has given rise to a modern field in chemistry (stereochemistry). Since optical activity in artificial chiral materials is a purely electromagnetic interaction, it is discernible over a wide range of frequencies by simply scaling the chiral element dimension to the appropriate excitation wavelength. To date, optical activity studies have been limited to the visible, near infrared, and microwave spectral regimes and little attention has been given to the terahertz (THz) range of the spectrum [17]. In addition, experimental investigations have focussed on illuminating optically active materials with continuous electromagnetic radiation and measuring the time-averaged intensity of either scattered or transmitted radiation. While continuous-wave measurements are very valuable, they tend to be very limiting when extracting the complex chiral material parameters. Unquestionably, since optical activity is an electric field phenomenon uniquely identified by its signature on the rotation of the plane of oscillation of the electric field and its ellipticity, it would be very advantageous to directly measure the LCP and RCP electric field components and their phases rather than inferring the information from intensity measurements. In this regard, direct time-domain investigation of amplitude, phase accumulation, propagation time, phase velocity, handedness, and polarization circulation of the electric field components, will help to shed light on the nature of the interaction process. Moreover, observation of transients of the optical activity over a temporal window will assist in developing better theoretical models, which have previously been restricted to the frequency-domain [18-25].

Almost two centuries have passed since optical activity was first observed and the intrinsic complexity of the interaction process has prevented an exact analytical description of the phenomenon in a helical chiral media [26]. To date, all theoretical models have straddled many simplified approximations that treat the chiral substance as a homogeneous isotropic effective medium governed by a set of averaged constitutive relations. To bring time-domain measurements into the helical optical activity dominion, one requires a means of irradiating the artificial helical chiral substance with an ultrashort electromagnetic pulse and capturing the electric field temporal evolution as the radiation is transmitted through the optically active medium.

This paper explores the THz optical activity of ensembles of dense randomly oriented metallic helices by studying their time-domain response to THz electromagnetic pulse excitation. The interaction of an electromagnetic wave with this artificial chiral material mimics the interaction with highly concentrated optically active macromolecules. By dynamically accessing the THz electric field transmitted through the helical chiral media, optical activity signatures are correlated with the arrival time and polarization state of the detected THz electric field radiation. We show that electromagnetic activity manifests itself as two distinct effects: one which is associated with local preferential scattering from individual helices and the other which is associated with collective coupling between individual chiral elements.

It merits a comment here that over a century has passed since Bose's remarkable experiment; it appears that we are following in his footsteps. While in 1898 Bose used a simple high voltage spark gap to generate mm/cm electromagnetic waves, we use an analogous system employing a solid-state optically triggered photoconductive semiconductor voltage switch for generating the THz radiation.

2. Experimental setup

To gain better insight into the intricate optical activity dynamics associated with chiral media, one requires new experimental tools in order to probe the polarization state. As depicted in Fig. 1, a polarization-sensitive THz time-domain spectroscopy setup is employed for performing the experiments. A semi-insulated GaAs photoconductive switch biased to 20 V_{p-p}

#108071 - $15.00 USD Received 26 Feb 2009; revised 31 Mar 2009; accepted 31 Mar 2009; published 6 Apr 2009

at a frequency of 54 kHz is employed as a THz emitter. Here, 1 ps, single-cycle, linearly polarized THz pulses are generated and detected using 20 fs, 800 nm pulses supplied from a Ti:sapphire Kerr-lens mode-locked laser. The THz pulses are collimated by a 5 cm focal length off-axis, gold-coated parabolic mirror. The optical beam from the Ti:sapphire laser is split into a weak 30 mW probe beam (used for the detection of the THz radiation) and a 250 mW pump beam (used for the generation of the THz radiation). To sample the THz waveforms, both the probe and THz beams are spatially overlapped and co-focused via a 20 cm focal length lens and another identical parabolic mirror, respectively, on a ZnSe <111> electro-optic detector [27]. The THz detection process is based on second-order nonlinearity using a non-centrosymmetric material. As the THz and optical probe pulses co-propagate in the <111>-oriented ZnSe electro-optic crystal, the electric field magnitude of the THz pulse is mapped onto the polarization state of the optical probe pulse via the THz electric field which modulates the index change. The THz pulse-induced phase change of the probe is converted into an intensity modulation that is proportional to the magnitude of the THz electric field by a quarter wave-plate and a polarizing beam splitter (Wollaston prism), and it is detected with a pair of photodiodes arranged in a differential detection mode. To access the cross-polarization states (parallel and perpendicular) of the THz electric field, the ZnSe crystal is reoriented by 90° depending on which component is to be measured. Since temporal overlap between the THz pulse and the probe pulse is required to measure the THz electric temporal waveform, a mechanical delay line is used to vary the time delay between the probe pulse and THz pulse, and the electric field waveform is recorded as a function of the sampling time delay.

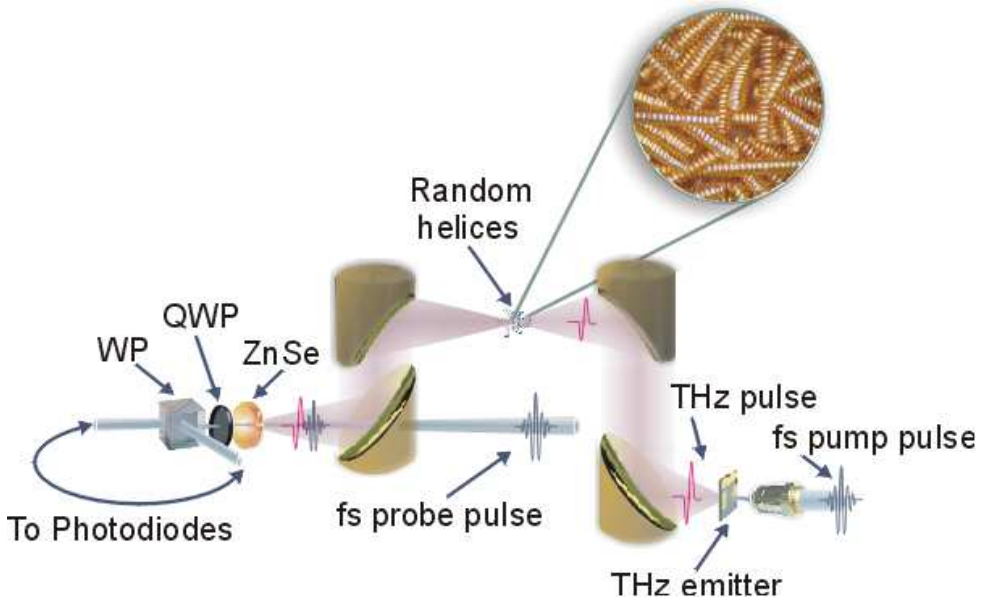

Fig. 1. Schematic of the THz time-domain spectroscopy setup (WP: Wollaston prism, QWP: quarter wave-plate). To access the cross-polarization states (parallel and perpendicular) of the THz electric field, the <111>-ZnSe electro-optic crystal is reoriented by 90° depending on which component is to be measured. Note that the photograph of the helices does not depict the random nature of the ensemble. The helices are piled-up for illustrative purposes only.

The artificial chiral media is composed of Au-coated Cu helices consisting of 17.7 right-handed circular revolutions, a winding pitch $K = 121 \pm 6\mu m$, a wire diameter $b = 60 \pm 2$ μm, and a helical centre-to-centre diameter $\delta_h = 295 \pm 5$ μm. At THz frequencies, the metallic helices are perfectly opaque to the radiation due to their large negative permitivity. Thus,

#108071 - $15.00 USD Received 26 Feb 2009; revised 31 Mar 2009; accepted 31 Mar 2009; published 6 Apr 2009

THz radiation of a wavelength λ_{THz} incident on the helical chiral ensemble is almost completely reflected, and some radiation is transmitted after it traverses the 2mm thick chiral ensemble.

Since a helical conformation exhibits not only optical rotation but also CD, a large CD response can make it difficult to discern the absolute rotation of the plane of polarization of the ellipse. However, since CD is shown to be maximum when the length of the metallic wire helix is half a wavelength [5,7,9,21], the effect of CD resonance absorption is minimized by choosing the helix length to be 2.07 mm (±0.02mm) (or an effective wire physical length of 16.6 mm >>λ_{THz}). Using a network analyser, we confirmed that absorption resonance for a single helix is 10.3 GHz, which is far away from the peak (0.4 THz) of the excitation spectrum of the THz pulse.

In order to construct a random chiral ensemble, 211 helices were packed into a 9.6mm×2.02mm (±0.02) mm×24.2mm polystyrene sample holder providing a 2.02 ±0.02mm thick random chiral medium for the THz radiation interaction. It should be noted that the thickness of the container is slightly less than the length of a single helix. While this may appear to influence the randomness of the sample, there were several other factors made in this choice, and this was found to be the best overall thickness. Initially, much thicker containers were considered, but transmission through these samples was very limited and meaningful results were either absent or obscured by noise. Containers which were slightly wider than the length of a helix were also considered, but it was found that a disproportionate fraction of helices settled in a way that is similar to logs stacked in a woodpile. Randomness was lost in such a sample and results would show strong influences of the axial modes propagating along the axis of these "stacked" helices. By considering a container slightly narrower (by only 4%) than the length of a helix, we were able to observe significant transmission (8%) through the ensemble. In addition, when the container was shaken to randomize the helices, it was observed that they settled in a highly random fashion. While no helices were able to settle in an axial orientation, there were some that settled in a very similar orientation. Axial modes in helices are well-understood [17] and it has been observed that the interaction process is substantially different than for other "random" orientations and would not contribute in any useful way to our study. This experiment was intended to investigate the analogy between a wire helix and a chiral molecule. As far as we know, there is no analogy to an "axial mode" in a chiral molecule, and we decided that this would not be detrimental to our results or analysis. In the end, we settled on a container width of 2.02 ±0.02mm. The container was shaken lightly for several seconds so that the orientation of each helix became randomized. Upon inspection, it was evident that through this process the helices became arranged in a wide variety of orientations and that an overall randomness was achieved. In such an array, all the helices are in contact with neighboring helices, and thus, the ensemble can be considered as an '*electrically*' interconnected right-handed chiral media. The sample holder was mounted on a 3D translation stage, and placed at the focal point between two 50.8 mm diameter, off-axis, gold-coated parabolic mirrors each having a focal length of 5 cm, as shown in Fig. 1. The spot-size of the beam at the incident side of the container was ~1mm. In order to ensure that a variety of possible random orientations were being explored and that the observations were representative of the material as a whole, a total of nine locations were considered. These measurements were taken on a 3×3 grid with point separations of 0.5mm in both the horizontal and vertical directions. Both parallel and perpendicular components of the transmitted field were recorded before translating the stage to the next spot. Transmission through the sample was found to be approximately 8.24% of the free space signal.

3. Experimental results and discussions

In these experiments, the optical activity of the chiral medium is probed by measuring the time evolution of the transmitted THz electric field pulse. Both components of the electric field are measured independently: the co-polarized, $E_{\|}(t)$ (parallel to incident THz electric

#108071 - $15.00 USD Received 26 Feb 2009; revised 31 Mar 2009; accepted 31 Mar 2009; published 6 Apr 2009

field pulse polarization), and cross-polarized, $E_{\perp}(t)$ (perpendicular to incident THz electric field polarization). From this orthogonal field vector set, the orthogonal LCP [i.e. $E_l(t)$], and RCP [i.e. $E_r(t)$], field components are constructed according to the following relations: $E_l(t) = 1/\sqrt{2}[E_{\parallel}(t) + iE_{\perp}(t)]$ and $E_r(t) = 1/\sqrt{2}[E_{\parallel}(t) - iE_{\perp}(t)]$. In this analysis, we adopt a convention of RCP and LCP as described by the rotation of the plane of polarization when the wave propagates towards an observer where RCP or LCP waves rotate in a clockwise or a counter clockwise direction, respectively. It should be noted that this is typically the convention used in the optics community, but that the opposite convention is often used in the antenna engineering community.

In order to calculate $E_l(t)$ and $E_r(t)$, it is necessary to phase shift the cross-polarized component by $\pi/2$ radians, and add or subtract it from the co-polarized component. In this fashion, the resulting LCP and RCP signals are represented as real value oscillating electric field components. While this is a straightforward implementation for continuous-time (multi-cycle) signal having a well-defined wavelength, it is more involved when dealing with a single-cycle pulse which contains a range of frequency components and does not have a well-defined wavelength. Rather than implementing this phase shift in the frequency domain or by simply advancing or delaying the cross-polarized components by a time constant, we employ the Hilbert transform to phase shift the pulse directly in the time-domain [28]. It is crucial to realize that this technique does not time-shift the entire pulse by a time constant. This technique effectively shifts localized regions of the wave separately.

Fig. 2(a) illustrates the averaged co-polarized, $E_{\parallel}(t)$ and cross-polarized, $E_{\perp}(t)$ and Figs. 2(b)-(j) depict the time-domain LCP and RCP electric field pulses captured after propagating through the helical chiral media. Represented in Figs. 2(b)-(j) are independent measurements at nine locations within the ensemble. The handedness of the chiral medium manifests itself in the interaction process. Evidently, since the chiral medium is right handed (composed of right handed helices), the LCP component of the electric field pulse is subjected to greater overall attenuation and scattering than the RCP electric field pulse. When the incident electric field vector is perpendicular to the helical axis, there is maximum absorption since a significant portion of the electric field vector is aligned along the wire surface. However, when the incident electric field vector is parallel to the helical axis, there is minimum absorption. For the random right-handed helical ensemble, the orientation of the helical axis is random relative to the THz electric field polarization. Nonetheless, the signature of CD is evident on the strong absorption for LCP electric field waveforms as illustrated in Fig. 2(k) which is averaged over the nine sampled positions.

Upon closer inspection of the time-resolved electric field waveforms, it is evident that the phase between the two circular components varies over the pulse duration. Better insight can be gained by examining the instantaneous phase difference, $\Delta\Phi(t) = \Phi_l(t) - \Phi_r(t)$ between the LCP and RCP the components of the pulse, where $\Phi_{l,r}(t)$ is the instantaneous phase of the RCP or LCP component, respectively. Notably, the variation of the phase shift with time corresponds to the instantaneous frequency, $\omega(t)=\partial\Phi/\partial t$.

The averaged $\Delta\Phi(t)$ over the nine probed locations is shown in Fig. 3. It should be noted that the same trend as shown in Fig. 3 is observed for each probed position. Within the time $0\text{ps} \le t \le 2\text{ps}$ after the pulse arrival (The pulse arrival time is characterized by the time at which the signal to noise ratio exceeds 10:1. This choice is in accordance with the common convention used to define the risetime to be the time taken for the pulse to rise from 10% to 90% of its amplitude), there is a noticeable phase difference as $\Delta\Phi(t)$ decreases from zero to –0.5 rad. The fact that the phase difference is negative indicates that the RCP electric field component is accumulating more phase than the LCP electric field component, or effectively, the refractive index for the RCP wave is larger than the LCP wave. However, this behavior is contrary to what is expected from the interaction of electromagnetic interaction with a chiral

#108071 - $15.00 USD Received 26 Feb 2009; revised 31 Mar 2009; accepted 31 Mar 2009; published 6 Apr 2009

substance. Since this chiral medium is right handed, it is expected that more phase is acquired by the LCP electric field component than by the RCP electric field

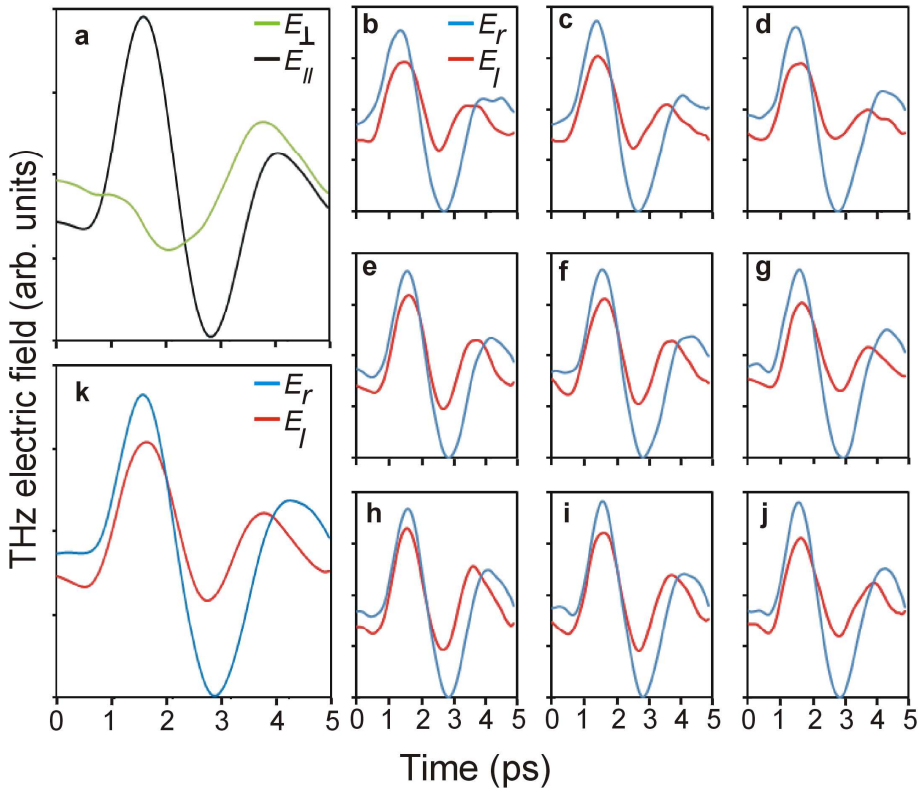

Fig. 2. (a) Time-resolved parallel $E_{\parallel}(t)$ (black) and perpendicular $E_{\perp}(t)$ (green)electric field pulse waveforms averaged over nine positions. (b)-(j) Time-resolved right circular $E_r(t)$ (blue) and left circular $E_l(t)$ (red) electric field pulse waveforms transmitted through the random ensemble of right-handed metallic helices. Each of the panels represents a sampling of a position in the chiral medium. (k) Time-resolved right circular $E_r(t)$ (blue) and left circular $E_l(t)$ (red) electric field pulse waveforms averaged over the nine positions.

Evidently, there must be an ultrafast interaction mechanism responsible for this phase accumulation. Within the time interval 2ps < t < 3ps, while $\Delta\Phi(t)$ is still negative, its magnitude decreases due to increased phase accumulation of the RCP wave. Beginning at time t = 3 ps, $\Delta\Phi(t) = 0$, and for the remainder of the pulse, $\Delta\Phi(t)$ begins to rise sharply in a nonlinear fashion. For the next 1.88 ps (until 4.88 ps after the pulse arrival), the LCP electric field component accumulates a significant phase of 4.36 radians relative to the RCP component.

#108071 - $15.00 USD Received 26 Feb 2009; revised 31 Mar 2009; accepted 31 Mar 2009; published 6 Apr 2009

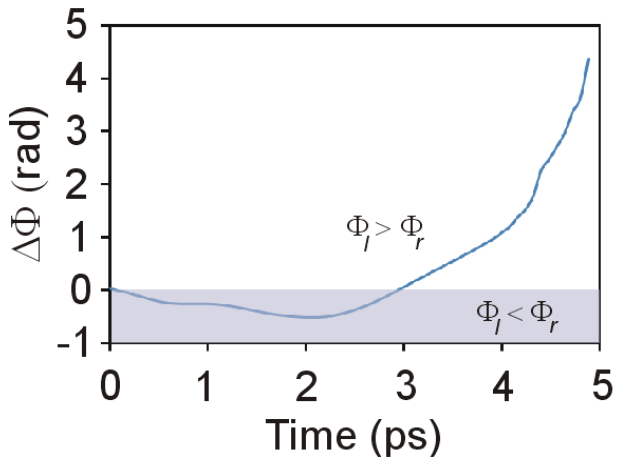

Fig. 3. The time-dependent phase difference between the LCP and RCP electric field pulse components transmitted through a 2mm thick random ensemble of right-handed metallic helices.

Interestingly, the delayed phase accumulation of the LCP electric field component suggests that the onset of the handedness-dependent refractive index cannot be an instantaneous process. Moreover, the nonlinear trend of the temporal delay appears uncharacteristic. A fundamental question arising would be: do such macroscopic artificial chiral media behave differently from their microscopic molecular counterparts? In a molecular chiral medium, both CD and ORD originate from the same electronic transitions, and they are governed by the causality of the Kronig-Kramer transformations, so the temporal retardation is nonexistent. In this regard, by accessing the time domain electric field, we are searching for new interpretations of the pioneering experiments by Lindman [5], Winkler [6], and Tinoco [7].

Since we are able to measure the magnitudes of the co- and cross-polarized components of the waves, the time-dependent trajectory of the tip of the electric field vector is plotted. As shown in Fig. 4, the right-handed chiral medium imparts its handedness on the transmitted THz wave sense of rotation. The temporal evolution of the CD and optical rotation are complex, and the presence of two distinct elliptical field trajectories (labeled A and B in Fig. 4) is evident. The ellipticity is a direct consequence of unequal magnitudes of $E_r(t)$ and $E_l(t)$. Within the first 2 ps, the electric field transforms itself from a state of linear polarization into an elliptically polarized state and for the remaining 2.88 ps, ellipse A evolves into a second ellipse B. The axial ratio (AR) of ellipse A can be computed from the ratio of maximum electric field, E_{max}, over the minimum field, E_{min}, (AR= E_{max}/E_{min} - obtained by dividing the magnitude of the major axis of the ellipse by the magnitude of the minor axis). The AR and the ellipticity, ε (= $\tan^{-1}(1/AR)$), are calculated to be 3.77 and 14.8°, respectively. However, within this time interval, ellipse A shows no noticeable optical rotation.

For t > 3ps, there is a significant change in the trajectory of the tip of the electric field. The plane of polarization of the ellipse is inclined by a large angle of ψ = 42°, forming a second polarization ellipse (ellipse B) with AR = 2.97 and ε = 18.6°. The large phase advancement of the LCP relative to the RCP electric field shown in Fig. 3 is the mechanism responsible for the observed rotation of the plane of polarization. Clearly, the observed optical rotation is not an instantaneous process. It should be noted that in continuous-wave intensity measurements (e.g. refs. 5-7,20,34,35), the measured circular dichroism, and optical rotation would have been due to the latter effect (i.e. polarization ellipse B) and the initial ultrafast temporal response would have eluded detection.

#108071 - $15.00 USD Received 26 Feb 2009; revised 31 Mar 2009; accepted 31 Mar 2009; published 6 Apr 2009

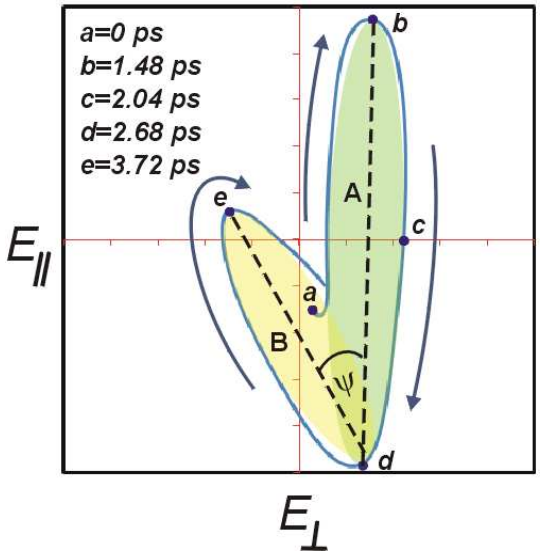

Fig. 4. Time-dependent trajectory of the tip of the electric field vector transmitted through a 2mm thick random ensemble of right-handed metallic helices. The locations a,b,c,d, and e denote the trajectory at different times.

To further shed light on the nature of the interaction process, we examine the instantaneous frequency contents of the transmitted LCP and RCP electric fields. By considering more elaborate digital signal processing techniques, this information becomes available via Wavelet transform. The Wavelet transform is capable of providing the time and frequency information simultaneously, hence giving an accurate time-frequency representation of the signal. Shown in Fig. 5(a) and Fig. 5(b) are the frequency-time maps of LCP and RCP electric field components, respectively, and their difference (i.e (RCP-LCP), Fig.5(c)). The signal can be decomposed into its frequency contents and in general, the amplitude of each frequency component varies with time. Figs. 5(a) and 5(b) illustrate how the relative weights (positive or negative values) of each frequency component vary in time. These are the individual frequency components (or wavelets) that need to be superimposed at different times to make up the whole signal. It is important to recognize that the LCP and RCP exhibit distinct spectral evolutions as indicated by the presence of significant frequency chirp. At t < 1.5 ps, the RCP electric field shows an initial up chirp as the low frequencies arrive earlier than the high frequencies. However, in the time interval 2 ps < t < 2.25 ps, all frequencies arrive at the same time (no chirp) as defined by a sharp transition edge. Note that at time t = 2 ps, $\Delta\Phi(t)$ is minimum (the phase difference between the LCP and RCP is minimum as shown in Fig. 3). At later times t > 2.25 ps the RCP electric field exhibits a significant frequency down chirp as high frequencies arrive earlier than the low ones. In contrast, at t < 2 ps, the LCP component exhibits no frequency chirp and beyond t > 2 ps a significant frequency down chirp is observed.

An important issue that arises is the origin of the temporal delay of the optical rotation. It is widely accepted that the interaction of the helical chiral media with the electromagnetic radiation can be analyzed from an electromagnetic perspective of coupled electric dipole and magnetic dipole moments. A simple picture illustrating the coupled dipole moments can be expressed in the following qualitative way [8,10,29-32]: Without a lack of generality, consider a single turn helix interacting with linearly polarized electromagnetic waves. Suppose that the artificial metallic helical macromolecule is oriented in a such way as to interact most strongly with the electric field, ***E(t)***, of the electromagnetic wave. When ***E(t)*** impinges on the metallic helix, the positive and negative charges are displaced in opposite directions within the skin

#108071 - $15.00 USD Received 26 Feb 2009; revised 31 Mar 2009; accepted 31 Mar 2009; published 6 Apr 2009

depth of the radiation (~70 nm at 1 THz). Thus, a dipole moment, ***P(t)***, whose magnitude is proportional to the electric field strength, is induced. However, the electric field interacts with different points along the helical turn, and along each location the helical perimeter constrains the charge motion to be along a helical path. Consequently, there is a circulatory displacement

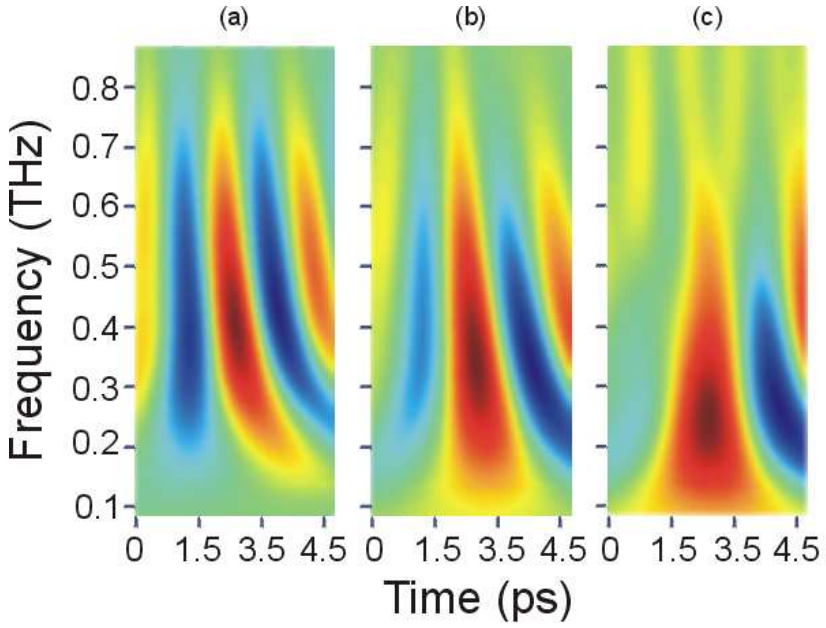

Fig. 5. Frequency-time maps of (a) LCP electric field component, (b) RCP electric field component, and (c) RCP-LCP electric field.

of the charges that manifests itself as time-varying helical currents that can be viewed as a combination of current along the ***E(t)*** direction, and that circulating around the ***E(t)*** direction. In turn, the circulatory current component induces a magnetic field, $\boldsymbol{H_{ind}(t)}$, or a magnetic moment, ***M(t)*****,** whose magnitude is proportional to $\partial E(t)/\partial t$. Alternatively, suppose that the metallic helix is oriented in a fashion that it interacts most strongly with the magnetic field of the electromagnetic wave, ***H(t)***. According to Maxwell's equations, the rate of change of the magnetic field, $\partial H(t)/\partial t$, through the helical loop induces an electric field $\boldsymbol{E_{ind}(t)}$ whose direction is defined by Lenz's law. Similarly, the induced positive and negative charge motion (or the induced magnetization currents) follows the same helical paths imposed by the helical turn. As a result, an electric dipole moment, ***P(t)***, is formed.

When the polarization direction of ***E(t)*** is perpendicular to the helical axis, there is maximum absorption since a significant portion of the electric field vector is aligned along the wire surface. However, when the incident ***E(t)*** polarization vector is parallel to the helical axis, there is minimum absorption. Here, the helix acts like a 'helical wire grid polarizer' selectively passing the radiation according to its orientation relative to the helix inclination. The differential absorption imposes the conditions required for observing CD, whereas the degree of coupling between ***P(t)*** and ***M(t)*** constitutes the rotation of the plane of polarization. Whether ***P(t)*** and ***M(t)*** are parallel or antiparallel, depends on the handedness of the helix. The ensemble average over all orientations gives rise to the effective chirality of the medium. This intuitive picture serves as the basis for modifying Maxwell's equation to include the two constitutive relations describing the interaction of electromagnetic waves with artificial chiral composites.

However, for the above-described analysis to be valid, the metallic helix must behave quasi-statically as an electrically inductive lumped element where the whole helix interacts

#108071 - $15.00 USD Received 26 Feb 2009; revised 31 Mar 2009; accepted 31 Mar 2009; published 6 Apr 2009

with the radiation fields at the same time over its entire length. This condition can only be implemented when the dimensions of the helix are less than one-tenth of the incident radiation wavelength such that field retardation effects are negligible. In our experiments, this condition is not satisfied since the helix length is 2.07 mm, which is larger than the probe terahertz radiation wavelength. In addition, the random chiral ensemble is dense where the metallic helices are touching each other (i.e. electrically interconnected). Moreover, the maximum electrical response of each individual helix making up the helical random media occurs at its natural resonance (10.3 GHz), measured using a microwave network analyzer. Excitation occurs at a much higher frequency (THz), and thus, an individual helical element cannot be considered electromagnetically active when treated as a lumped circuit equivalent element. That is, since magnetic dipole moments are produced by flowing charges, the helix's large inductance and reactance make it too slow to respond instantaneously to the driving ultrafast THz electric field. Currents cannot be induced fast enough to make the helix react instantly to the impinging ultrafast THz radiation. Thus, when the electromagnetic picture discussed above is invoked, the helix cannot be considered electromagnetically active and will not exhibit optical rotation when excited.

Since the coupled electric and magnetic dipole moments model is inadequate, one must invoke a faster mechanism that does not involve electric or magnetic dipole currents in order to describe the temporal behavior of the chiral medium. To this end, the helical media can be considered to be a random distribution of macroscopic scatterers, where each helical turn is essentially a microscopic conducting chiral scatterer. When the helix length is $> \lambda_{THz}$, its pitch and diameter are $\leq \lambda_{THz}$, and the helical chiral element interacts with the THz radiation in a fashion resembling light scattering from helically oriented point scatterers. Light propagating through the helical chiral media experiences both absorption and scattering processes, and thus the measured CD is the sum of both effects. It is important to distinguish between scattering and absorption when interpreting the transmitted light and the observed CD. It has been shown that, depending on its handedness, a macro-sized helix preferentially scatters either LCP or RCP light waves [33-38]. This phenomenon, known as circular differential scattering, occurs when a circularly polarized light wave with handedness matching that of the helix scatters preferentially in the forward direction, whereas a circularly polarized wave having the opposite handedness scatters to the side direction. The preferential forward and side scattering arises from the phase difference of light scattered from different segments on the helix.

In this regard, the overall observed optical activity can be explained to arise from local interactions and inter-helix coupling. Here, each point on the helical arc acts as an independent point scatterer to the incident light. The scattered light is a result of radiation emitted by changes in the local charge distribution induced by the THz electromagnetic field. This interaction process is instantaneous as it only requires inducing local current sources. Effectively, the current-induced polarizability of the chiral elements possesses the symmetry properties necessary for the differential scattering of light. Within the time $t < 2$ps, we observe that the $E_l(t)$ component experiences less phase buildup than the $E_r(t)$ component. This implies that the LCP wave travels faster in the medium than the RCP wave. When the LCP electric field component interacts with a right handed helix, it scatters off with preserved polarization that is opposite in handedness to the helices. That is, the transiently-induced local current sources radiate LCP fields that propagate through the right handed chiral media in a ballistic manner since coherent coupling between independent radiators is hindered by the helical conformation. Even though the LCP electric field component is side-scattered, the THz detection system acceptance angle of 53.1° is large enough to collect the side-scattered LCP radiation. This LCP wave arrives early as it does not interact and couple efficiently with the helices, and suffers minimum phase build up. However, the RCP electric field component interacts and couples more efficiently to the right handed chiral helices, where the locally-induced surface current sources radiate RCP electric fields more efficiently. Coherent

#108071 - $15.00 USD Received 26 Feb 2009; revised 31 Mar 2009; accepted 31 Mar 2009; published 6 Apr 2009

coupling between individual helices occurs and is cumulatively enhanced as the RCP wave propagates through the right handed chiral media. The observed delayed CD and optical rotation is attributed to nonlocal interaction. Due to the close packing of the helices, near-field coupling and interference between the scattered THz fields from individual helical loops couples the local electromagnetic fields. This mechanism is not instantaneous but it takes time to build up as the fields propagate, scatter, and couple between adjacent helices. In such a process, significant phase is accumulated by the RCP electric field as it is favorably coupled with the right-handed helices in comparison to the LCP electric field component. It is this interaction mechanism that is responsible for the observed delayed optical activity signature (as noted by ellipse B in Fig. 4).

4. Conclusion

Using terahertz time-domain spectroscopy, we investigate the optical activity arising from structural asymmetry of an artificial composite material consisting of randomly-oriented metallic helices. Time-domain measurements provide an additional degree of freedom in optical activity investigation. By accessing the temporal dynamics and polarization states of the electrical field wave forms transmitted through the chiral media, the temporal electric field trajectory can be mapped and sense of handedness, ellipticity, and optical rotation are measured directly. This experiment illustrates various aspects of the interaction in the time-domain and optical activity signatures marked by circular dichoism, differential circular scattering, and optical rotation are demonstrated. These effects are correlated with the phase accumulation/advancement between the LCP and RCP electric field components. We show that for this macroscopic metallic chiral medium, the electromagnetic interaction cannot arise from coupled electric and dipole moments, but must be due to a combination between local preferential circular scattering from individual helices and collective coupling between individual helices. These two effects are distinctly separated in time.

Although this experiment was carried out in an artificial chiral media, these findings can possibly serve as a prelude to time and angularly-resolved experiments involving optically active macromolecules. Since the circular differential scattering pattern is directly related to the configuration asymmetry and the critical dimension of the interacting macromolecules, it is envisioned that this unique application of THz time-domain spectroscopy will arise.

Acknowledgments

This work was supported by the Natural Sciences and Engineering Research Council of Canada (NSERC) and the Canada Research Chairs (CRC) program.

#108071 - $15.00 USD Received 26 Feb 2009; revised 31 Mar 2009; accepted 31 Mar 2009; published 6 Apr 2009